

2018



**25th Congress of
International Federation for
Heat Treatment and Surface Engineering**

11-14 September 2018 | Xi'an China

PROCEEDINGS



Organized by Chinese Heat Treatment Society (CHTS)

25th IFHTSE CONGRESS PROCEEDINGS

11-14 September 2018

Xi'an China



Chinese Heat Treatment Society

Tel: +86 (0) 10 6292 0613 • Email: chts@chts.org.cn • Web: www.chts.org.cn

Add: 18 Xueqing Rd., Beijing, China

Study on aging heat treatment and stability control of aluminum alloy engine block.....	70
Quench sensitivity of Al-7Si-0.2Mg high pressure vacuum die cast alloy.....	70
Hot deformation induced evolution of the precipitations in an Al-Li alloy.....	71
Improvement of fatigue strength of carburizing steel 20MnCrS5 during carburizing quenching.....	71
Effects of solution and aging treatment on reverse austenite in 174PH stainless steel.....	72
Phase transition of two-dimensional oxide crystal from topological phase to perovskite.....	74
Parameters optimization design of quenching and partitioning based on artificial neural network and particle swarm optimization.....	76
Effect of two-step Q&P treatment on microstructure and mechanical properties of 65Si2MnWA steel.....	78
Microstructure of retained austenite and its strengthening toughening mechanism in 300M steel.....	80
Effect of dissociated NH ₃ Gas at the several of filament temperatures in the gas nitriding.....	82
Effect of annealing process on mechanical properties of tungsten-rhenium alloy wires.....	84
Effect of cold rolling on mechanical properties of Al-0.1Sc-0.05Zr alloy during solution aging.....	85
Changes of microstructure and mechanical properties of 6061 aluminum alloy by friction stir processing under different heat treatment conditions.....	86
Latest developments of deep cryogenic treatment.....	87
Study on plasma spraying process and corrosion resistance of NdFeB alloy surface.....	88
Formation of coherent microstructure with cuboidal nanoprecipitates in BCC-based high-entropy superalloys and their microstructural stability.....	89
Grain refinement and mechanical properties of a Fe-30Mn-0.11C steel.....	89
Studies on attractive MoAlB ceramics: hot pressing sintering process and its high temperature oxidation resistance.....	90
Development of walking beam furnace for forging heating aluminum alloy billet of wheel hub.....	90
Heat treatment effects on the microstructure and mechanical properties of 11Cr-3Co-2.3W martensitic heat resistant steel.....	91
The process optimization of organic-inorganic hybrid perovskite thin film.....	91
Effect of heat treatment process on ZrW ₂ O ₈ synthesis by hydrothermal method.....	91

Chemical-thermo Treatment

The effect of oxy-nitriding on the corrosion resistance of AISI 304 austenitic stainless steel in H ₂ S environment.....	92
Distortion control technology for large-size and thin-wall carburizing and quenching gear.....	93
Effect of the deformation on carbonitriding microstructure of the cold deformed Ti-6Al-4V alloy.....	94
Nitrogen expanded austenite with superior load-bearing capacity: microstructure control and formation mechanism.....	95
Future trends in gaseous surface hardening of titanium and titanium alloys.....	96
Prestudy on mechanical property of dual-phase microstructure in X100 pipeline steel.....	97

Atomistic diffusion mechanism of rare earth carburizing/nitriding on iron-based alloy.....	98
Effects of depositing atmosphere on microstructure, mechanical and tribological properties of titanium nitride film.....	99
Low temperature surface hardening; from fundamental understanding to predicting composition and stress profiles.....	100
Three-dimensional reconstruction of composite microstructures.....	100
Surface properties of diamond-like carbon in-situ growth on Fe ₃ C-containing carburized layer by plasma carburizing.....	101
Mechanical properties and microstructure evolution of borided hot-work tool steel.....	101
Rare earth doping and alloying mechanism during plasma nitrocarburizing of low-alloy steel.....	102
Enhancement of thermal fatigue resistance for H13 steel by low temperature plasma nitriding.....	102
Effect of alloy cations on corrosion resistance of LDH/MAO coating on magnesium alloy.....	103
Effect of zirconium addition on hot corrosion behavior of chromium-aluminium coating on nickel-based superalloy.....	103
Application of isothermal transformation to the formation of a nitrided layer.....	104
Effect of oxidation temperature on gas oxygen, nitrogen, carbon composite processing layer corrosion resistance.....	104
Experimental study and first-principles calculations of carbon “expanded” α phase on stainless steel surface.....	105
Troubleshooting HeaAkin Malast-treatment furnace atmospheres and new control technologies to avoid problems.....	105
Surface catalytic behavior of ABO ₃ type perovskite compounds during gas nitriding with rare earth addition.....	106
Microstructure and properties of composite surface modified layer fabricated on 6061 aluminium alloy by surface mechanical nano-alloying combined with nitriding treatment.....	106
Microstructure evolution and mechanical properties of nitride/aluminide coatings prepared by plasma nitriding Ti-coated 2024 Al alloys.....	107
Faster carburizing speed in nitrogen methanol atmosphere with injection lances.....	107
Influence of NH ₃ flux on CrN precipitation during low temperature plasma nitriding of AISI304 austenitic stainless steel.....	108
The evolution of microstructure forecast and test for carburizing and quenching 17CrNiMo6 steel.....	108
A study of modifying (La,Sr)(Co,Fe)O ₃ surface by plasma glow discharge.....	109
Quantitative analysis of solid solute in Zr-2.5Nb alloy by ATP technique.....	109
Effect of rare earth La on microstructure and properties of niobium carbide coating on H13 steel.....	110
Study on formation mechanism of surface nanocrystalline layer during plasma nitriding of steel.....	110
Quenching deformation control of ZL205A aluminum alloy by in situ formation of high strength gradient multiphase layer.....	111

Surface grain nanocrystallization of Fe-Cr-Ni alloy steel by plasma thermo-chemical treatment.....	111
Boriding treatment on alloyed white cast irons.....	112
Rolling contact fatigue behavior of carbonitrided AISI 52100 high carbon bearing steel.....	113
Evaluation of thermal fatigue property of surface-modified SKD 61 steel by gas nitriding and shot peening.....	114
Thermal fatigue evaluation of AISI H13 steels surface modified by gas nitriding with pre- and post-shot peening.....	115
Microstructure and properties of plasma nitrided layer of aerospace TC4 alloy.....	115
Electronic structures of InGaN ₂ nanotubes.....	116
Applications of XD super nitriding activator.....	116
Preparation and properties of nano-TiN co-deposited Ni-P composite coatings on TL084 copper alloy.....	117
Low temperature plasma hardening of long and thin stainless steel tubes in the nuclear reactor.....	117

Heat Treatment and Surface Engineering for Key Parts and Components Industries

Microstructure and corrosion resistance of Ni-based alloy coated onto gray cast iron using a multi-step induction cladding process.....	118
Effects of the induction heat treatment on microstructure and properties of hot rolled stainless steel clad plate.....	120
Synchronized vacuum heat treatment for fully integrated manufacturing lines and small batch treatment.....	122
Effects of pulse current on tensile deformation behavior of pure titanium.....	123
Precipitation behaviour of μ phase in new type Co-base superalloys.....	124
Quenching behaviour of a high wear resistant Cr-rich cast alloy.....	125
Effects of fiber coating on interfacial reaction and mechanical properties of SiC _f /Ti composites.....	126
The oxidation behaviour of NiCrAlYSi coatings at 1100 °C by arc ion plating.....	127
Microstructural evolution and mechanical properties of Ti-6Mo-5V-3Al-2Fe alloy aged at various temperatures.....	128
Weight-efficient powertrain components—steel grades, heat treatments and performance.....	129
Techniques to improve the performance of Hadfield steel frogs.....	130
Increase efficiency and productivity using Tubothal elements and Kanthal APM™ radiant tubes.....	131
Endothermic generator design and reactions.....	132
Case hardening by low pressure carburizing in highly efficient emicontinuous vacuum furnaces.....	132
Application of DSP Intelligent induction heating power supply in induction heat treatment fields of key parts.....	133
Cost- and resource effective surface layer heat treatment in gear and tool industry by PulsPlasma®-nitriding.....	133

The effect of oxy-nitriding on the corrosion resistance of AISI 304 austenitic stainless steel in H₂S environment

Longyi Li¹, Jun Wang¹, Hongyuan Fan¹, Hanshan Dong², Jun Cao³, Guiyang Wu³

(1. College of Manufacturing Science and Engineering, Sichuan University, Chengdu, China;

2. School of Metallurgy and Materials, University of Birmingham, Edgbaston, Birmingham B15 2TT, UK;

3. Research Institute of Natural Gas Technology, PetroChina Southwest Oil and Gas Field Company, China)

Srwanjun@scu.edu.cn

Abstract: H₂S is one of the most dangerous factors causing metal corrosion in acidic oil and gas environments, and electrochemical corrosion will occur on the surface of the pipeline. In addition, natural gas pipelines are also exposed to wear and corrosion caused by the sand and mud carried by the airflow. So it is necessary to take some strengthening measures to improve its surface strength on the premise of ensuring its good comprehensive performance. The aim of the present paper is to study the effect of low-temperature liquid bath nitriding on the corrosion resistance of AISI304 austenitic stainless steel in the H₂S environment.

The raw materials used in this experiment were non-toxic cyanate, chloride and carbonate salts. The nitriding process involved immersing the sample in 723 K molten salt for 8 h, during which the non-toxic cyanate decomposes into carbon atoms and nitrogen atoms, forming a high chemical potential on the surface of the sample. The H₂S corrosion test was adopted the solution 'A' recommended by NACE TM0177-2005. Both the untreated and nitrided samples were soaked in this solution for 720 h.

Before and after the experiment, the mass of the sample was weighed and recorded. Therefore, the corrosion weight loss rate was calculated. The uniform corrosion rate is calculated as follows: $R_{\text{corr}}=8.76 \times 10^4 \times (m-m_0)/(S_1 \times \rho \times t)$. OLYMPUS GX51 optical microscope and JSM-7500F scanning electron microscope were used for microstructural analysis. The surface phase structure was tested using an EMPYREAN X-ray diffractometer (XRD). The SHIMADZU-1720 electron probe microanalyzer (EPMA) was used to quantitatively analyze the elemental distribution from the surface to the matrix. XPS analyses were carried out with a XR3E2 apparatus from Vacuum Generator.

Nitriding produced 3-layered structure consisting of an oxide top layer, a nitrided layer and a carburized layer. Under the same conditions, the thickness of the nitrided layer is greater than that of the carburized layer. A number of etch pits and crack were observed on the surface of the untreated sample, which indicates pitting and crevice corrosion of the sample; while the nitrided samples showed no significant change after H₂S corrosion. The corrosion rate of the untreated 304 austenitic stainless steel (0.2006 mm/a) is approximately 3.6 times the average weight loss after nitriding (0.0557 mm/a).

The XRD patterns clearly show S-phase peaks, indicating that the S-phase layer is successfully produced during nitriding. The corrosion product of the untreated sample is Fe_{1-x}S, while the corrosion products of the nitrided samples were mainly Fe₇S₈, Fe_{1-x}S, and Fe₂O₃.

EPMA results of the untreated and low temperature nitrided samples show oxygen concentration increased significantly in the nitrided layer due to introduced oxygen atoms during nitriding process. The concentration of nitrogen was increased due to the formation of supersaturated austenite.

XPS analysis results showed that the corrosion products of untreated and nitrided samples were approximately the same, mainly Fe₂O₃, FeOOH. Besides, S content and Fe content of the untreated sample are significantly larger than that of the nitrided sample, which shows that nitriding can prevent the formation of corrosion products on the surface of the sample. Nitriding layer is supersaturated with active nitrogen atoms, which combine with H⁺ to avoid surface pH reduction, thus decelerating H₂S corrosion.

Low-temperature liquid nitrided samples have better corrosion resistance than untreated samples in H₂S environment. The corrosion products are mainly consisted with oxides, hydroxides, and sulfates. Nitriding layer reduces the production of corrosion products; further corrosion of the sample is prevented.

Keywords: austenite stainless steel, oxy-nitriding

Distortion control technology for large-size and thin-wall carburizing and quenching gear

Zhonghe Zhang, Feiyu Wang, Quanzhen Wang, Erkang Zhang, Yang Guo, Tianlong Cui, Yanzhao Geng
(Shenyang Blower Works Group Corporation, Shenyang 110869)
goingabroad201412@163.com

Abstract: 12Cr2Ni4 (17CrNiMo6, 18CrNiMo7-6), the C-shaped distortion test sample and the scaled down simulate gear were individually used as test material and distortion test tools for the practice problem of large distortion and complicated distortion on large-size and thin-walled carburizing quenching gears on blower. The effects of pre-heat treatment method, the uniformity of material composition, the method of quenching after carburizing and the dimensions of gear structural on distortion were analyzed by a large number of experimental studies. In particular, the impact of structural size on distortion was systematically tested and combined with metallographic microstructure analysis. The following rules are obtained: triangle law of distortion: the number of process holes is designed in multiples of 3, the distortion is greatly reduced, that is, the triangle stability principle is still applicable to anti-distortion; the golden section law design: the relationship between the circumferential diameter of the process hole and the gear diameter, the distortion is greatly reduced when the golden section law is applied; the optimum value and the maximum rule: for the ratio of the diameter to the thickness of the gear designed, there is an optimum value on anti-dimensional distortion, the ratio is 10, and there is a maximum in the anti-elliptical distortion, the ratio is 11; equal diameter rule: the lifting hole and the process hole is designed to equal in diameter, which could greatly reduce elliptical distortion; controlling the uniformity of raw material composition, using the quenching and tempering in the pre-heat treatment and using once quenching method instead of twice quenching method, the distortion could be greatly reduced.

Finally, “one straight line and two curves” macroscopic solution were raised in this paper. “One straight line” was the directly solve the carburizing and quenching distortion. “Two curves” was a roundabout tactic. The first one was adopted simplified process to reduce the distortion of carburizing and quenching. The second one was to replace the carburizing and quenching with ion nitriding and avoid the problem of distortion. the method of designing large-size thin-walled carburizing and quenching gears, the method of the pre-heat treatment and the inspection of controlling the uniformity of the compositions are proposed. The distortion of the gear carburizing and quenching could be greatly reduced, the uniformity of carburizing layer thickness and surface hardness, the hardness distribution are evenly improved. The contact fatigue strength and bending fatigue strength of the carburizing and quenching gears are also greatly improved. In addition, the innovation test on international conventional C-type samples is used and the new C-type sample which the sensitivity raised up 30% is invented.

Keywords: carburizing and quenching, distortion control

Effect of the deformation on carbonitriding microstructure of the cold deformed Ti-6Al-4V alloy

Yudong Fu¹, Huanzheng Sun², Yang Song²

(1. Chinese Heat Treatment Society; 2. Harbin Engineering University)

fuyudong@hrbeu.edu.cn

Abstract: Ti-6Al-4V (TC4) alloy is the most widely used titanium alloy in the world, under the comprehensive consideration of the existing carbonitriding and the technology of promote the carbonitriding, the surface modification of TC4 alloy is achieved by a composite technology of solution treatment+cold rolling+500 °C pulsing plasma carbonitriding, explore the effect of carbonitriding on the microstructure of the alloy. The comparison technology is nitriding or aging treatment. The transformation of deformed microstructure, carbonitriding microstructure of the alloy and the infiltrated layer were characterized successively by scanning electron microscopy (SEM), EDS energy spectrum analysis, X-ray diffraction analysis (XRD), microhardness test, and friction and wear test.

The metallographic and scanning test results show that the Ti-6Al-4V alloy layer treated by carbonitriding consists of compound layer and diffusion layer, the microstructure grains are obviously refined with the increase of deformation. EDS energy spectrum analysis results show that the main composition of the compound layer is TiN phase, while the diffusion layer is composed of TiN, Ti₂N, and TiC phases. The aging precipitation phase gradually increases with the increase of the deformation; with the prolongation of the holding time of the carbonitriding treatment, the content of the β phase in the matrix of the infiltration layer continuously increases. The proportion of nitrogen-titanium and carbon-titanium atoms in the compound layer of the alloy decreases with the deformation of the sample increases. The increasing trend of the nitrogen and titanium content of the infiltrated layer gradually slows down, because the ion concentration deviation between the surface layer and the substrate of the sample increases, a large number of surface excited ions are infiltrated into the matrix through lot of defects in the sample, and few excited ions in the chamber are bound to the titanium atom of surface layer. Microhardness test data showed that the hardness of the alloy treated by carbonitriding increased by 100% approximately; the hardness of the cross-section from the outermost to the matrix gradually decreased, and the hardness of the matrix was higher than the untreated sample by about 30%; combined with the results of energy spectrum analysis, it can be seen that the N and C elements infiltrated in the deformed alloy are in a gradient distribution, the hardness of the alloy is increased and the gradient weakening rule is maintained. Friction and wear test data show that compared with nitriding or aging treatment technology, the wear coefficient and volume wear rate of the TC4 alloy specimen after carbonitriding treatment are reduced obviously, after 30% deformation sample carbonitriding 22 h, the volume wear rate decreased by 65% and the friction coefficient was below 0.6 and all lower than the untreated sample. With the alloy deformation increase and the time of carbonitriding prolonged, the wear mechanism of the sample has changed from adhesive wear to abrasive wear. The presence of nitrogen and carbide hardening phases in the surface layer of the sample resulted in greatly improvement of the friction and wear properties of the alloy.

Keywords: Ti-6Al-4V alloy, carbonitriding, composite process

Nitrogen expanded austenite with superior load-bearing capacity: microstructure control and formation mechanism

Bo Wang, Marcel A. J. Somers
(Technical University of Denmark)
bo.win@outlook.com

Abstract: Austenitic stainless steels are extensively used in the chemical and food industries due to their excellent corrosion resistance. However, the inherently low surface hardness and poor wear resistance have restricted their applications in engineering fields. A practical approach for solving such a difficulty is to prepare expanded austenite on austenitic stainless steel by dissolving high amounts of nitrogen (or carbon) in the austenite phase through low-temperature nitriding (or carburizing) process.

In recent years, low temperature gas nitriding has become one of the most widely used technology to prepare expanded austenite due to the convenient operation, strong process controllability and geometrical constraints. However, low temperature nitriding is usually applied as a finishing step after a series of metal forming operations to shape the stainless product, the martensite induced before would cause the precipitation of nitrides during gas nitriding. Moreover, the load-bearing capacity of the thin modified layer with single expanded austenite is not satisfactory due to its intrinsically brittle nature and the plastic deformation of the substrate of austenitic stainless steel.

In this research, a multi-step surface treatment of high temperature solution nitriding, surface severe deformation and low temperature gas nitriding is proposed to rapidly prepare a precipitates-free nitrogen expanded austenite layer on austenitic stainless steel. The process involves first preparing a stable austenite layer with a low interstitial nitrogen content through solid solution nitriding to prevent strain-induced martensite formation during surface plastic deformation treatment, and then refining the grain size and inducing dislocations to accelerate nitrogen diffusion by the subsequent surface deformation, followed by low temperature nitriding. The effect of combined treatment on the formation and the microstructure characteristics of nitrogen expanded austenite is investigated. After the multistep surface treatment, a thicker nitrided layer consisting of the pure expanded austenite layer and the subsurface deformed zone can be formed. The nanocrystalline surface layer induced by surface severe deformation caused high chemical activity and rapid diffusion of nitrogen due to the large number of grain boundaries and abundant defects. The combined process can provide the technical basis for rapid preparation of outstanding expanded austenite layer, serving as a driving force for the development of surface engineering of stainless steels where the expanded austenite zone is supported by a high load-bearing capacity.

Keywords: expanded austenite, austenitic stainless steel, gas nitriding, surface severe deformation

Future trends in gaseous surface hardening of titanium and titanium alloys

Thomas L. Christiansen, Morten S. Jellesen, Marcel A. J. Somers

(Technical University of Denmark, Produktionstorvet b.425 DK 2800 Kongens Lyngby, Denmark)
tch@mek.dtu.dk

Abstract: Titanium is a light weight highly corrosion resistant material used in many different industries such as aerospace, biomedical, military and chemical processing. Titanium is also biocompatible and is one of the materials of choice for implants and medical devices. Furthermore, it is widely used in 3D metal printing, which is becoming increasingly popular in industry. One of the major shortcomings of titanium (and its alloys) is its poor wear resistance, which hinders a more widespread use of the material in applications involving wear. Surface engineering is the classical way to improve the wear performance of materials, but for the case of titanium, this is not trivial due to titanium's very strong affinity to interstitially dissolvable elements. The present contribution presents new gaseous thermochemical routes for surface hardening of titanium and its alloys.

The first part addresses new methods for gaseous low temperature surface hardening of titanium by incorporation of interstitial oxygen. It will be shown that relatively deep and hard diffusion zones of oxygen in solid solution can be obtained by chemically controlled low-partial pressure oxidation. The second part presents new routes for high temperature gaseous surface hardening of titanium; in particular emphasis is given to so-called mixed interstitial solid solutions and compounds in the Ti-based system. Combinations of different interstitial elements give rise to unique and intriguing materials properties and behavior, such as enhanced solubility in titanium and faster growth rates. The surface hardness can be tailored in the range 1500 to 3000 HV and case depths beyond 0.5 mm can be achieved. It is envisaged that these new types of low and high temperature surface hardening processes will pave the way for more widespread use of titanium and its alloys in the future.

Keywords: titanium, surface hardening

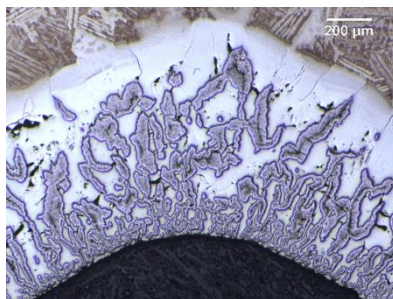


Fig.1 Micrograph of surface hardened titanium grade 2; mixed interstitial phases

Prestudy on mechanical property of dual-phase microstructure in X100 pipeline steel

Danli Zhang¹, Yuanbin Qin¹, Qinqin Fu¹, Jiming Zhang², Zhiwei Shan¹

(1. Center for Advancing Materials Performance from the Nanoscale, State Key Laboratory for Mechanical Behavior of Materials, Xi'an Jiaotong University, Xi'an 710049, China;

2. China National Petroleum Corporation Tubular Goods Research Institute, Xi'an 710077, China)
zhangdanli20054731@126.com

Abstract: Pipeline transportation is an important way for long distance transportation of crude oil and natural gas. Recent years, more and more efforts have been put on the research on X100 pipeline steel due to its good application prospect.

The present work aims to distinguish ferrite and bainite present in X100 pipeline steel and determine mechanical properties of dual-phase microstructure via nano-indentation using Hysitron's TI950 Tribo-Indenter and compression test with PI87 Pico-Indenter in SEM which is useful in material design.

Nano-indentation result reveals that the reduced modulus of the sample is about 200 GPa. The average hardness of bainite and ferrite is quite different, which is about 4.45 GPa for bainite and 3.42 GPa for ferrite.

Compression of ferritic and bainitic pillars fabricated by focused ion beam shows that the engineering stress of ferritic pillars is almost the same with that of bainitic pillars, seen as Fig.1. Strength of bainitic pillar is about 600 MPa and ferritic pillar is around 700 MPa. We can see obvious slip during the compression of bainitic pillars, but no obvious slip during the compression of ferritic pillars. Considering the grain size and the size of pillars, we speculate that there must be only one grain in a ferritic pillar. But in bainitic pillar there may be two or more grains, so relative sliding may occur between grains under stress. The compression of ferrite and bainite mixed pillars shows similar results to the compression of bainitic pillars, shown in Fig.2.

Keywords: mechanical properties, pipeline steel

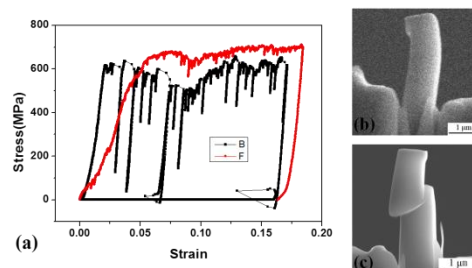


Fig.1 (a) Stress-strain curves of ferritic and bainitic pillars; SEM images of (b) ferritic and (c) bainitic pillars after compression.

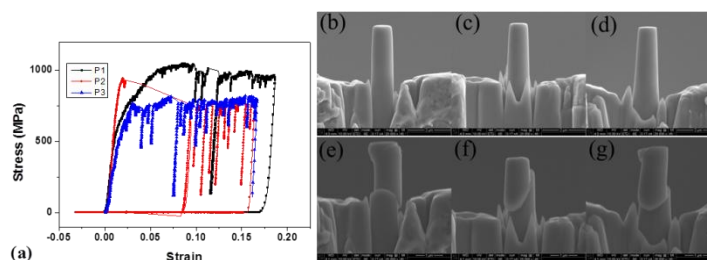


Fig.2 (a) Stress-strain curves of ferrite and bainite mixed pillars; SEM images of pillars (b), (c), (d) before compression and after compression (e), (f), (g)

Atomistic diffusion mechanism of rare earth carburizing/nitriding on iron-based alloy

Yuan You¹, Mufu Yan², Jihong Yan²

(1. Qiqihar University; 2. Harbin Institute of Technology)

greatyouyuan@163.com, yanmufu@hit.edu.cn

Abstract: Nitriding and carburizing are important methods to strengthen the surface of iron-based alloys. Addition of rare earth (RE) during nitriding or carburizing will reduce processing time, increase thickness, improve microstructures and mechanical properties of modified surface layers. A modified surface layer with high strength and good toughness is obtained by RE-nitriding or RE-carburizing. There are extensive applications for RE-nitriding and RE-carburizing in experimental researches and industrial manufacture. However, the researches on RE catalyzing, strengthening and toughening mechanism during nitriding or carburizing on iron-based alloys are seldom reported. Therefore, first-principles calculations are employed to investigate RE-nitrided and RE-carburized layers on iron-based alloys in this work. Our investigations focus on solid solution and surface of bcc Fe with alloying elements such as C, N, La, Al, Si, Ti, V, Cr, Co, Ni, Cu, Nb and Mo. Our calculated results are summarized as follows.

1) The atomistic diffusion mechanism of C and N atoms in iron-based alloy is illuminated. Interaction energy of two FIAs (foreign interstitial atoms) first nearest neighboring to each other reaches to 2.32 eV, and they repel to each other. The concentration gradient of C (or N)+the repulsion of FIAs = the resultant force towards core of C (or N) atoms. The resultant force towards core is the diffusion driving force of N (or C) atoms in iron-based alloy.

2) The RE catalyzing mechanism is discovered. i. The diffusion driving force of N (or C) atoms is enhanced. Interaction energy of La and N (or C) nearest neighboring to each other reaches to 2.34 eV (2.70 eV). The diffusion driving force of N (or C) atoms in nitriding (or carburizing) is the repulsion. The diffusion driving force of N (or C) atoms in RE-nitriding (or RE-carburizing) is the repulsion of N (or C) atoms + the La-N (or -C) repulsion. ii. The implantation of N (or C) atoms into the iron surface due to RE adsorption. Because of the adsorption of RE, N (or C) atom moves from on the surface (0.65 Å or 0.76 Å) to into the surface (0.01 Å or -0.01 Å). iii. The RE catalyzing anti-trip theory is developed. The octahedral interstitials are the trips of N (or C) atoms. In RE-nitriding (or -carburizing), RE atoms occupy the points of crystal lattices, and substitute Fe atoms. An anti-trip zone around a RE atom is formed due to the La-N (or -C) repulsion. Because of the existence of many anti-trip zones, the concentration of N (or C) increases rapidly. Furthermore, the increase of N (or C) concentration gradient accelerates the diffusion of N (or C) atoms.

3) The strengthening and toughening mechanism of RE-nitriding (or -carburizing) is proposed. i. The bonding strength of N (or C) atom and its neighbor Fe atoms is enhanced on account of RE addition. When a La atom is introduced and is the first or second nearest neighboring to N (or C) atom, the Fe-N (or -C) bond populations increase, and the strength of the covalent bond increase. ii. With RE addition, the compressive stress increases and the microstructures are refined. When a La atom occupies a substitutional site, the relaxations of Fe atoms 1-4 nearest neighboring to La are 6.2%, 2.5%, 0.6% and 0.2%.

These relaxations are significantly greater than other alloying elements.

In our investigations, the RE catalyzing, strengthening and toughening mechanism of RE-nitriding (or -carburizing) is proposed. This work is beneficial to technological innovation of RE-nitriding (or -carburizing), design, preparation and application of RE doped and modified new materials. Our calculation results and proposed theory are of significance to theoretical studies and applications.

Keywords: atomistic diffusion mechanism, rare earth, carburizing, nitriding, iron-based alloy

Effects of depositing atmosphere on microstructure, mechanical and tribological properties of titanium nitride film

Shidong Zhang

(National Key Laboratory for Precision Hot Processing of Metals,
School of Materials Science and Engineering, Harbin Institute of Technology)
stone_hit@163.com

Abstract: The purpose of this study is to investigate the effect of depositing atmosphere on microstructure, mechanical and tribological properties of titanium nitride film.

Prior to deposition, the substrates needed to be polished till the root mean square surface roughness was less than 0.1 μm . Then these polishing surfaces were ultrasonically cleaned in acetone for 15 min, in ethanol for 10 min to clean the grease contamination and in deionized water for 5 min to remove residual liquid. Then there are three depositing steps of TiN film. First, the bias voltage of the substrate was adjusted to -400 V for ion cleaning for 30 min in order to remove the surface oxides and to activate surface, and the Ti target current was adjusted to 0.3 A. Second, the Ti underlayer was deposited onto the substrates at a Ti target current of 5.5 A for 20 min with a substrate bias of -70 V. In the above two steps, high purity argon gas (99.99%) was introduced to control the process pressure of 4.0×10^{-3} Torr and argon flow was 16 sccm. Third, the TiN layer was deposited with the Ar/N₂ ratio of 1:1, 1:2, 1:3, respectively and its deposition time was 360 min.

TiN film was prepared on synchronizing rings using a unbalanced magnetron sputtering system. The so-obtained film was then characterized by grazing incidence X-ray diffractometer (GXRD), scanning electron microscopy (SEM), atomic force microscopy (AFM), nanoindentation tests and ball-on-disk tribometer.

The TiN film surface was uniform, smooth and dense which was mainly composed of Ti and N element. The roughness (R_q) of TiN film obtained a minimum of 9.85 nm, when the ratio of argon to nitrogen was 1:1. While the ratio of argon to nitrogen was 1:2, the R_q obtained a maximum of 67.5 nm. XRD analysis showed that the as-prepared film only had ZnCu phase and TiN phase. At the Ar/N₂ ratio of 1:1, the XRD diffraction peak of TiN phase was more obvious. Compared with the untreated substrate, the COF of coated one increased and its wear rate decreased. The COF of untreated substrate was about 0.12, the COF of coated one was about 0.12, 0.23 and 0.14, corresponding to the Ar/N₂ ratio of 1:1, 1:2, 1:3 respectively. The wear rate of untreated substrate obtained a maximum of 6.571×10^{-7} g/(N r), whereas the wear rate of coated one was about 2.321×10^{-7} , 1.429×10^{-7} and 1×10^{-7} g/(N r), corresponding to the Ar/N₂ ratio of 1:1, 1:2, 1:3, respectively. Compared with the untreated substrate, its corresponding wear rate was reduced by 65%, 78% and 85% respectively.

TiN coating significantly improved the mechanical and tribological properties of synchronizing rings. Increasing the proportion of argon in the mixed gas within a proper range can promote the growth of the TiN film and reduce its surface roughness, the friction coefficient and the wear rate. The film had the best tribological and mechanical performance when the ratio of argon to nitrogen was 1:1.

Keywords: TiN film, mechanical, tribological

Low temperature surface hardening; from fundamental understanding to predicting composition and stress profiles

Marcel Somers

(DTU)

somers@mek.dtu.dk

Abstract: The case developing during low temperature surface hardening of austenitic stainless steel by nitriding, carburizing or nitrocarburizing consists of a supersaturated interstitial solid solution of nitrogen and/or carbon in austenite. The favorable properties of this so-called expanded austenite depend on the profiles of interstitial concentration and associated composition-induced residual stress over the case. The prediction of composition and stress profiles for a certain steel grade from the process parameters gas composition, temperature and treatment time would enable targeted surface engineering of stainless steels. Furthermore, such a numerical model would enable the design of new stainless steel grades that are tailored for optimal performance during low temperature surface hardening, equivalent to the well-known nitriding steels. Preferably, such a numerical model departs from the state of knowledge of microstructure evolution in order to arrive at accurate predictions. For this purpose the availability of fundamental parameters as determined experimentally on homogeneous powders and foils under well-defined conditions is essential.

In the present contribution an overview of the current state of understanding of the evolution of the microstructure, composition and residual stress during low temperature surface hardening of stainless steels is presented. The presentation showcases the joint achievements of many co-workers in the last 18 years. The overview concerns theoretical, experimental and modelling aspects of expanded austenite, both as a homogeneous phase and as a case on stainless steel. The topics covered are:

- 1) Interstitial solubility, interstitial diffusion and phase stability of homogeneous expanded austenite;
- 2) Crystallography, thermal expansion and magnetism of homogeneous expanded austenite;
- 3) Origin, measurement and tailoring of residual-stress in expanded austenite cases;
- 4) Numerical prediction of composition- and growth and thermal stress profiles with a diffusion model that incorporates the interaction of composition and stress as well as the elasto-plastic accommodation of composition-induced lattice expansion.

Keywords: stainless steel, thermochemical surface engineering, fundamentals, modelling, residual stress

Three-dimensional reconstruction of composite microstructures

Yanxiang Zhang

(Harbin Institute of Technology)

hitzhang@hit.edu.cn

Abstract: X-ray computed tomography (XCT) is well-known to the reconstruction of three-dimensional (3D) microstructures of composites, however, not available in most research institutions. Here we present a new technology based on distance correlation functions, capable of reconstructing the 3D microstructures from a single 2D micrograph. This method is verified using XCT datasets. Demonstrative 3D reconstruction combining with specially designed experiments is proposed employing (La,Sr)MnO₃-YSZ composites. This technology is general for reconstructing a wide range of composite microstructures, and permits deep understanding of microstructure-property relationship.

Keywords: 3D reconstruction, microstructure

Surface properties of diamond-like carbon in-situ growth on Fe₃C-containing carburized layer by plasma carburizing

Yang Yang, Mufu Yan, Yanxiang Zhang
(Harbin Institute of Technology)
yanmufu@hit.edu.cn

Abstract: The article reports a valuable finding of diamond-like carbon (DLC) film in-situ growth on Fe₃C-containing carburized layer by plasma carburizing. The microstructure of the carburized layers coated with and without DLC film was compared and analyzed by means of optical microscope, scanning electron microscopy (SEM) equipped with energy dispersive X-ray analyzer, atomic force microscopy (AFM), X-ray diffraction (XRD), Raman spectroscopy and X-ray photoelectron spectroscopy (XPS). The tribological tests demonstrate that the DLC film growing on the carburized layer has lower frictional coefficient and wear rate compared with traditional carburized layer, which attributes to self-lubricating property and high nano-hardness (13.227 GPa), respectively. This study successfully combines DLC deposition and preparation of carburized layer into a single-step process, which explores the potential of plasma carburization in DLC production.

Keywords: diamond like carbon, plasma carburizing, in-situ growth, lubricating, wear

Mechanical properties and microstructure evolution of borided hot-work tool steel

Undrakh Mishigdorzhijn, Nikolay Ulakhanov
(ESSTUM)
druh@mail.ru

Abstract: This research investigates the effect of high-temperature boriding from slurries on mechanical properties and microstructure of hot-work tool steel. The treatment was conducted at furnace heating for 4 h at 1100 °C. Boron carbide powder was chosen as a boron supplier, sodium fluoride - as an activator. In addition, aluminum powder was added to boriding agent. Powder components were mixed and kneeled with acetone and organic glue. It was discovered, that the use of boriding temperatures over 1000 °C results in the layer formation with composite structure, where iron borides FeB and Fe₂B evenly distributed in the matrix of aluminum solid solution in iron. It was also established, that the microhardness profile has no sharp slope due to deep transition zone. The wear resistance of the treated samples was tested by means of pin-disk method. The results indicated that high-temperature boriding improves wear resistance of hot worked tool steel. The composite structure contributes significantly to the mechanical properties of the layer; in particular, it enhances its wear resistance.

Keywords: thermochemical treatment, case hardening, boriding, treatment slurries, microstructure, microhardness, wear resistance, composite-structured diffusion layer, hot-work steel

Rare earth doping and alloying mechanism during plasma

nitrocarburizing of low-alloy steel

Yixue Wang, Mufu Yan

(Harbin Institute of Technology)

sunnywang2013@sina.com, yanmufu@hit.edu.cn

Abstract: Rare earth (RE) elements usually promote the kinetics of thermal chemical treatments (such as plasma, gas nitriding, carburizing, and nitrocarburizing processes), refine the microstructure and toughen the multi-component permeation layer. However, it is not clearly known that why the RE elements can promote these kinetics and improve the malleability. In present work, a highly efficient method has been applied to enhance the kinetics of nitrocarburizing for medium carbon steel by introducing RE elements, such as La. By comparing with the ordinary counterpart, the interplays between the RE elements and the matrix elements, such as Fe, C, were analyzed in terms of phase composition, elements valence and chemical composition examinations. We demonstrated that the thickness of RE nitrocarburized layers is increased by a factor of 44.23% as compared to that by the ordinary nitrocarburizing process. A strong bonding effect of La-N by XPS, combining with the offset γ' -Fe₄N peaks in XRD patterns were detected, demonstrating that La atoms could incorporate into the γ' -Fe₄N lattice and form γ' -(Fe, La)₄N on the nitrocarburized surface. This new phase was further confirmed to be γ' -(Fe, Al, La)₄N by the first-principles calculation. In addition, LaFeO₃ was formed on the surface, which was the most likely candidate to effectively promote the decomposition of dense compound layer (usually the main obstacle for N diffusion), thus providing abundant paths for N atom diffusion. γ' -(Fe, Al, La)₄N and LaFeO₃ on the nitrocarburized surfaces inhabited the ϵ -Fe₃N formation from the energetic viewpoint, which was the main obstacle for N diffusion. Elastic constants calculation results indicated the toughness increase without serious compromise of the strength for the RE nitrocarburized layer, which resulted from the decomposition of the brittle ϵ phase. All the results demonstrated a promising potential of RE elements as novel catalyst for the high efficiency nitrocarburizing.

Keywords: plasma nitrocarburizing, rare earth, catalyst

Enhancement of thermal fatigue resistance for H13 steel by

low temperature plasma nitriding

Jing Hu, Yao Chen, Tiantian Peng

(Changzhou University)

jinghoo@126.com

Abstract: A self-designed test for evaluating the thermal fatigue resistance was developed according to the cooperator's requirements, and plasma nitriding at lower temperature was conducted for H13 steel to improve its thermal fatigue resistance in this study. The treated samples were characterized by optical microscopy (OM), X-ray diffraction (XRD), microhardness tester and a self-designed thermal fatigue test. The results show that a nitriding layer with only diffusion zone was formed on the surface while nitriding at low temperature of 470 °C for 8 h. Meanwhile, the thermal fatigue resistance was greatly enhanced and brittleness was significantly decreased due to no compound layer existed at the outmost zone while nitriding at lower temperature.

Keywords: H13, thermal fatigue resistance, plasma nitriding

Effect of alloy cations on corrosion resistance of LDH/MAO coating on magnesium alloy

Junfeng Chen¹, Linchi Zou², Wenxin Lin¹

(1. Fuzhou University; 2. Fujian University of Technology)

chenjunfeng@fzu.edu.cn, zoulinchi@fjut.edu.cn

Abstract: Micro-arc oxidation (MAO) can improve corrosion resistance of magnesium alloys, but it significantly restricts the promotion of corrosion resistance due to the existence of pore and micro crack. In this study, three types of LDH/MAO coating were prepared via covering layered double hydroxide (LDH) on MAO pre-treated AZ31 alloy, and the effects of these three types of LDH on the corrosion resistance of AZ31 alloy were investigated for the first time. Detailed morphology and composition of the LDH/MAO coatings were characterized using scanning electron microscopy (SEM), X-ray diffraction (XRD), and X-ray photoelectron spectroscopy (XPS). Besides, the corrosion resistance of AZ31 alloy with different LDH/MAO coatings was also tested by electrochemical work station. The results from polarization curves and electrochemical impedance spectroscopy show that AZ31 alloy coated with Ni-LDH/MAO has the higher impedance modulus and lower corrosion current density than Zn-LDH/MAO and Al-LDH/MAO. The Ni-LDH/MAO coating remarkably improved anti-corrosion of AZ31 alloy during long-term immersion in 1 M NaCl solution, since Ni-LDH film can completely cover the original MAO coating and effectively adsorb a large number of NO₃⁻ to exchange Cl⁻ in corrosion solution.

Keywords: alloy cations, magnesium alloys, layered double hydroxide, corrosion resistance

Effect of zirconium addition on hot corrosion behavior of chromium-aluminium coating on nickel-based superalloy

Mohamed Elhelaly¹, Mohamed El-Zomor¹, Mohamed Hussien¹, Ahmed Osman Youssef²

(1. Tabbin Institute for Metallurgical Studies; 2. Faculty of Science-Ain Shams University)

melhelaly2018@yahoo.com

Abstract: Nimonic 75 alloy was coated with two different types of coatings; Cr-Al coating this is called aluminizing-chromizing and Zr-doped Cr-Al coating this is called aluminizing-chromizing-zirconizing. Diffusion coating was carried at 1000 °C for 8 h under atmospheric pressure by simultaneous aluminizing-chromizing process and by simultaneous aluminizing-chromizing-zirconizing. The microstructures and hot corrosion behavior of the coatings were characterized using LOM, SEM/EDS and XRD. The cyclic hot corrosion tests of Nimonic 75 and its coated system deposited with 3-5 mg/cm² Na₂SO₄ were conducted at 900 °C in air for 150 hrs at 10 hrs cycle. The results indicate that Zr-doped chromium aluminium coating is more effective in increasing the hot corrosion resistance of Nimonic 75 alloy. The role of zirconium can be attributed to an improvement of the adherence of the oxide scales. In addition, the distribution of elements and precipitates within the coatings and the substrate before and after the hot corrosion tests was analyzed. From this investigation, some suggestions were made for better hot corrosion resistance of the coatings.

Keywords: Nimonic75, hot corrosion, pack cementation process, superalloys, diffusion coating

Application of isothermal transformation to the formation of a nitrated layer

Piotr Nawrocki, Jerzy Szawłowski
(Institute of Precision Mechanics)
piotr.nawrocki@imp.edu.pl

Abstract: The article presents the effect of the isothermal quenching process on forming of the microstructure and properties of the nitrated layer on two types of steel with different carbon content, i.e. 0.02 and 1.08, and alloy additions such as tungsten, chromium and molybdenum. Gas nitriding process was conducted at the temperature of 550 °C for 30 h. After the nitriding process, steels were subjected to austenitizing and isothermal quenching for four variants of temperature and time parameters, i.e. two austenitizing temperatures: 750 °C and 860 °C/50 min, and two isothermal quenching temperatures: 390 °C and 420 °C/2 h. For low austenitizing temperatures, the possibility of nitrogen austenite formation was assumed, while a higher temperature should lead to the formation of austenite saturated with carbon and nitrogen.

The paper presents the microstructure of the layers by using light microscopy and scanning electron microscopy (SEM), the cross-section hardness distributions measurements and the determination of internal stress of layers by $\sin^2\psi$ method.

Keywords: nitriding, isothermal transformation, internal stress, nitrogen austenite

Effect of oxidation temperature on gas oxygen, nitrogen, carbon composite processing layer corrosion resistance

Mian Wu¹, Lin Pan¹, Xiangyang Tong¹, Tongzhou Chen¹, Fei Ma^{2,3}

- (1. Wuhan Research Institute of Materials Protection, State Key Laboratory of Special Surface Protection Materials and Application Technology, Wuhan 430030, China;
2. Qingdao Branch of China Academy of Mechanical Science & Technology, Qingdao 266000, China;
3. The Project National United Engineering Laboratory for Advanced Bearing Tribology, Henan University of Science and Technology, Luoyang 471000, China)
whpl61@sina.com

Abstract: In this paper, the gas oxygen, nitrogen, carbon composite treatment of 40 Cr steel and H13 steel layer of Tafel polarization curve measurement, soak test and salt spray test, we analyzed the effect of oxidation temperature on layer corrosion resistance. The results showed that as the temperature rises, the corrosion potential of the sample first increases and then decreases. With the increase of oxidation temperature, sample immersion test corrosion rate gradually increases. With the increase of temperature after salt spray test specimens appear in rust is gradually reduced. Gas nitrocarburizing 400 °C by 1 h oxidation treatment of the sample for better corrosion resistance.

Keywords: gas oxygen, nitrogen, carbon composite treatment, oxidation temperature, corrosion resistance

Experimental study and first-principles calculations of carbon “expanded”

α phase on stainless steel surface

Ruiliang Liu, C. Y. Wei
(Harbin Engineering University)
liuruiliang@hrbeu.edu.cn

Abstract: In the present investigation, AISI 431 stainless steel was low temperature plasma carburized at 430 °C for different times to prepare carbon “expanded” α (α' C) phase layer. The microstructures of the layers were characterized by optical microscope and X-ray diffraction. The mechanical properties of the layers were characterized by nanoindentation tester. The α' C phase were treated as nominal molecular formula of $\text{Fe}_{13}\text{Cr}_3\text{C}_x$ ($x=0, 2, 4, 6$), then the stability, electronic structure and mechanical properties were calculated by using the density functional theory (DFT) within the generalized gradient approximation (GGA). Experimental results show that there are the uniform layers on stainless steels after plasma carburized at 430 °C for different times. The layer thicknesses on stainless steel plasma carburized for 4 h, 8 h and 16 h are about 25 μm , 38 μm and 46 μm , respectively. The surface phases are mainly of α' C phase with a small amount of Fe_3C phase. The surface hardness of the carburized specimen is up to 15 GPa. The elastic moduli of 4 h, 8 h and 16 h carburized specimens are about 278 GPa, 200 GPa and 176 GPa, respectively. The calculation results indicate that carbon atoms incline to locate in the octahedral interstice structure without Cr atoms. For $\text{Fe}_{13}\text{Cr}_3\text{C}_x$ ($x=0, 2, 4, 6$) structure, with the increasing of carbon content, the structural and mechanical stabilities decrease gradually, the hardness value increases first and then decrease, the elastic moduli decreases from 230 GPa to 66 GPa, while the toughness would increase gradually based on B/G values evaluation. All the calculated results are almost in agreement with the experimental results.

Keywords: stainless steel, low temperature carburizing, “expanded” α phase, nanoindentation, first-principles calculation

Troubleshooting HeaAkin Malast-treatment furnace atmospheres and new control technologies to avoid problems

Akin Malas
(Linde North America LLC)
akin.malas@linde.com

Abstract: Heat treatment is still considered a “black art” as process parameters cannot always be fully controlled and sometimes can only be predicted. Many of the expected theoretical reactions may, in fact, not occur. Practical methods for monitoring and controlling furnace atmospheres can limit problems and help achieve more consistent parts quality.

By analyzing the thermochemical reactions and considering the cause-and-effect relationships based on experience with the process may help operators avoid many atmosphere-related problems. There are also new technologies available to address issues which may traditionally be considered unavoidable, such as checking the integrity of methods for furnace-atmosphere analysis or atmosphere-gas circulation to achieve uniformity. The paper will present practical methods to approach these issues and detail new control technologies.

Keywords: new control technologies, furnace atmospheres

Surface catalytic behavior of ABO₃ type perovskite compounds during gas nitriding with rare earth addition

Xing Chen, Chengsong Zhang, Guodong Cui
(Southwest Jiaotong University)
cszhang@swjtu.edu.cn

Abstract: In present work, the gas nitriding was carried out with rare earth addition in order to obtain a thick nitrided layer on the surface of steels in a short time. The rare earth was added by prefabricating a thin film on the surface of steels using the sol-gel method. The effect of process parameters (temperature, time and ammonia flow) on the microstructure of rare earth nitrided layer was investigated and the catalytic mechanism of rare earth was discussed. The microstructure and phase composition of rare earth nitrided layer were characterized by optical microscope (OM), scanning electron microscope (SEM) equipped with energy dispersive X-ray spectroscopy (EDS), transmission electron microscope (TEM), X-ray diffraction (XRD) and micro-hardness tester. The X-ray photoelectron spectroscopy (XPS) was used to identify the catalytic mechanism of rare earth by analyzing the chemical state on the nitrided surface. The results show that an ABO₃ type perovskite compound will form after gas nitriding, which results in the increase of nitrided layer thickness. The catalytic efficiency of ABO₃ type perovskite compounds depends on the process parameters. The optimal nitriding parameter was confirmed as 550 °C for 4 h. The ABO₃ type perovskite compounds could accelerate the nitriding rate by adjusting the ratio of the adsorption nitrogen atoms and absorbed nitrogen atoms. When the adsorption nitrogen atoms and absorbed nitrogen atoms meet a certain proportion of 1:1, it exhibits an obvious catalytic function.

Keywords: gas nitriding, surface catalytic behavior, rare earth, mechanism

Microstructure and properties of composite surface modified layer fabricated on 6061 aluminium alloy by surface mechanical nano-alloying combined with nitriding treatment

Jian Sun, Liangyu Mei, Yi Li, Xiaodong Du, Yucheng Wu
(Department of Materials Science and Engineering, Hefei University of Technology)
ycwu@hfut.edu.cn

Abstract: In this paper, a composite surface modified layer fabricated on 6061 aluminium alloy by surface mechanical nano-alloying (SMNA) combined with nitriding treatment. The microstructure, hardness and elastic modulus of composite surface modified layer were investigated by scanning electron microscope (SEM) equipped with energy dispersive X-ray spectrometer (EDS), X-ray diffraction (XRD), microhardness tester and nano-indenter. Experimental results showed that a nanostructured Fe alloying layer with thickness of 50-70 μm was fabricated on 6061 aluminium alloy by SMNA treatment. After nitriding at 450 °C for 6 h, a composite surface layer composed of Fe₂N/α-Fe(N)/α-Fe/Al phases was formed on SMNAed sample. The surface hardness of composite surface modified layer is approximately 589 HV and decreased slowly to the substrate value. In addition, the variation of elastic modulus of composite surface modified layer display gradient descent tendency from surface to substrate.

Keywords: 6061 aluminium alloy, surface mechanical nano-alloying, nitriding, composite modified layer, surface properties

Microstructure evolution and mechanical properties of nitride/aluminide coatings prepared by plasma nitriding Ti-coated 2024 Al alloys

Fanyong Zhang¹, Mufu Yan², Fuxing Yin¹, Jining He¹

(1. Hebei University of Technology; 2. Harbin Institute of Technology)

fany_zhang@163.com

Abstract: Transition metal nitride coatings usually showed large hardness difference and elastic mismatch with soft substrate, thus leading to fracture failure. In this study, a novel Ti-N/Ti-Al based multilayer design was developed to enhance surface mechanical properties of 2024 Al alloys. The Al alloy substrates were firstly deposited with pure Ti film by using magnetron sputtering and then plasma nitrided at different temperatures (400-490 °C) under N₂H₂ atmosphere. The microstructure evolution and mechanical properties of as-obtained coatings were investigated by using X-ray diffractometer (XRD), scanning electron microscopy (SEM), microhardness tester and pin-on-disc tribometer. Results showed that the multilayer coating was composed of three sublayers (i.e. the outmost TiN_{0.3} layer, the intermediate Al₃Ti layer and the inside Al₁₈Ti₂Mg₃ layer) at nitriding temperature higher than 460 °C. The surface hardness of 2024 Al alloy was remarkably improved by multilayer coatings, reaching a maximum value of 500 HV at 490 °C, which was about 8 times higher than that of the uncoated alloy. The friction coefficients of 2024 Al alloy decreased in the coatings prepared at higher nitriding temperature, reaching the lowest values of 0.31 at 490 °C. The wear rate of the coated samples decreased by 56% compared with the uncoated ones. The analysis of worn surface indicated that the nitrided samples exhibited severe adhesive wear at 400 °C that changed to predominant abrasive wear at increased nitriding temperature.

Keywords: nitride coatings, magnetron sputtering, plasma nitriding, multilayer structure, mechanical properties

Faster carburizing speed in nitrogen methanol atmosphere with injection lances

Zhijun Jiang¹, Xuwei Ning¹, Lei Shi², Xiaojia Ren²

(1. Airliquide (China) R&D Co., Ltd.; 2. Airliquide (China) Holding Co., Ltd.)

jim.jiang@airliquide.com

Abstract: The conventional gaseous carburizing process was mostly carried in about 20%CO atmosphere with the 40/60 nitrogen and methanol ratio or 23%CO generated from 1/7.5 propane and air. In this article, the researchers investigated the case depth and hardness profiles with different CO content from the typical carburizing cycle in the batch furnace. The carburizing atmosphere was adjusted by mass flow controller (MFC) with different nitrogen and methanol ratio and homogeneously sprayed into furnace by the injection lance. The main components of atmosphere (CO, H₂, CO₂, CH₄) were real-time measured and recorded by IR multi-gas analyzer. And combined with O₂ probe, the real carbon potential (C_p) can be calculated out and sent to controlling software or PLC.

New two-stage carburizing cycle was designed in this article with raised CO% to 25%-30% at the boost stage, and normal CO% at 15%-20% at the diffusion stage. The results showed the raised CO% with higher carbon transfer coefficient and lead to faster carburizing or the cycle time reserved with required case depth. The residual CH₄ content can be controlled below 0.5% even in the more than 25%CO atmosphere with the help of injection lance. The mass flow controller and injection lance were successfully applied in nitrogen-methanol atmosphere to directly generated wide range of CO content. It would help the gaseous carburizing more flexible and efficient.

Keywords: faster carburizing, nitrogen methanol atmosphere, injection lance, mass flow controller

Influence of NH₃ flux on CrN precipitation during low temperature plasma nitriding of AISI304 austenitic stainless steel

H. T. Chen¹, M. F. Yan²

(1. School of Materials Science and Engineering, Harbin University of Science and Technology, China;

2. National Key Laboratory for Precision Hot Processing of Metals,

School of Materials Science and Engineering, Harbin Institute of Technology, China)

htchen83@163.com

Abstract: Low temperature plasma nitriding was performed on AISI304 austenite stainless steel at different NH₃ flux and it was found that NH₃ flux will affect the microstructure and properties of the nitrided layer. Morphology and microstructure results reveal that higher NH₃ decreases the amount of chromium nitrides precipitation in the nitrided layers indicated by the less ‘dark’ areas. The XRD results showed that higher NH₃ flux favors to inhibit or delay precipitation of CrN and ϵ -Fe₂₋₃N, but promotes the formation of γ -Fe₄N in the modified layers. The results from potentiodynamic polarization experiments indicated deterioration or improvement of corrosion resistance at lower or higher NH₃ flux, respectively. The CrN and ϵ -Fe₂₋₃N precipitation at lower NH₃ flux is attributed to the higher density of the stack faults in the S phase induced by higher sputtering rate at low pressure. The stack faults provide the crystal nucleus for Fe₂₋₃N formation and enhance the probability of Cr movement and segregation. The remained ‘dark’ areas in the nitrided layer at higher NH₃ flux are explained by the undetected CrN precipitation and available Cr loss in the type of ternary compounds in Fe-Cr-N system.

Keywords: plasma nitriding, austenitic stainless steel, AISI 304, precipitation

The evolution of microstructure forecast and test for carburizing and quenching 17CrNiMo6 steel

Dengyu Gai, Yuanzhao Chu, Guang Cai, Yueyi Wang

(College of Materials Science and Chemical Engineering, Harbin Engineering University)

1293240994@qq.com

Abstract: 17CrNiMo6 steel is a kind of the high-strength low carbon alloy steel used for gears steel. Carburization and quenching are often applied for better performances. The process of carburizing and quenching is complex. Computer-aided material engineering and experiments were used in this paper to forecast and measure microstructure of 17CrNiMo6 steel during the carburizing and quenching. The distribution of carbon content in the material after carburizing was calculated using JMatPro, which is a software for thermodynamic calculation. And based on that, the chemical composition of different layers as well as properties calculation were achieved. Use the finite element software to simulate the temperature field of quenching process and then get the tissue distribution after quenching. Through the performance–temperature field–performance–microstructure iteration method, and comparing the simulation results with the experimental results, it can provide a reference for the evolution of microstructure forecast and text for carburizing and quenching 17CrNiMo6 steel.

Keywords: 17CrNiMo6 steel, carburization, microstructure forecast

A study of modifying (La,Sr)(Co,Fe)O₃ surface by plasma glow discharge

Jingbo Ma

(Harbin Institute of Technology)

jclarke1992@163.com

Abstract: Solid oxide fuel cells (SOFCs) is an clean and efficient device that could transfer chemical energy to power. Recent years intermediate temperature solid oxide fuel cells (IT-SOFCs) attracts researcher as lower temperature brings lower cost and higher durability. It is a significant problem to improve the rate of reaction on the surface of cathode. In this paper a plasma glow discharge method is used for the first time to improve the oxygen reduction reaction (ORR) of cathode. The electric conductivity relaxation method (ECR) and distribution of relaxation time (DRT) is applied to characterize the reaction rate of ORR. A better method is proposed to calculate DRT from electrochemical impedance spectrum (EIS). In the paper we adopt plasma glow discharge method to modify the surface of LSCF and coat nano-scale particles on the surface. The oxygen reduction reaction of the surface is promoted. The hollow cathode of Ni/Cu/Fe is used as target. The atmosphere of H₂/Ar is plasma and through bombarding metal atoms is coated on the surface. Samples are placed in the hollow cathode and as a result the metallic atoms deposit on the surface.

Because of the catalytic performance of transition metal, Ni/Cu/Fe are chosen as target. The relation between the treatment factors (time and temperature) and morphology of film is discussed. As time goes, the size of particles increases and the amount of particles increases. As temperature increase, the size of particles trends to increase. In lower temperature, lower valent metal oxide is preferred. The morphology of coating nickel and iron is column and while coating copper, the morphology is sphere and polygonal. Through changing the factors, the morphology of coating Ni/Cu/Fe could be controlled. The former works provides methods for modifying LSCF on the cell.

The optimized treatment of coating nickel is characterized by electrical conductivity relaxation methods and the surface exchange coefficient is proved to be improved by a magnitude. The formula which represents the control of bulk transport in LSCF is given. Later the mechanism of distribution of relaxation time is optimized, which has a higher resolution and provide powerful ways to characterize the surface process. Considering the resolution and robustness of the method, the optimized factors is obtained. The Gauss method is used to calculate the EIS data of LSCF in different temperature and the process limiting the performance of LSCF is shown.

Keywords: plasma glow discharge, nanostructure

Quantitative analysis of solid solute in Zr-2.5Nb alloy by ATP technique

Xue Liang

(Institute of Materials, Shanghai University)

liangxue@shu.edu.cn

Abstract: β -Nb precipitates are general second phase particles in Zr-Nb series alloys which are used as structural materials in nuclear industry. In this study Zr-2.5Nb alloy was investigated by atom probe tomography (APT). Focus ion beam sectioning technique was performed for APT characterisation sample preparation. Result shows that Fe segregates at the interface of β -Nb particles and α -Zr matrix, as well as at the grain boundary. The maximum segregation concentration appears at the point where Zr content is approximately equal to Nb content. But not all interface of β -Nb particles are enriched with Fe. Nb concentration in α -Zr matrix in this study is 0.67 at%.

Keywords: β -Nb, APT, segregation

Effect of rare earth La on microstructure and properties of niobium carbide coating on H13 steel

Jian Shang¹, Jun Xiang², Pan Zheng²

(1. Materials Science and Engineering College, Liaoning University of Technology;

2. National United Engineering Laboratory for Advanced Bearing Tribology)

shangjian@lnut.edu.cn

Abstract: The niobium carbide coatings are prepared by packing method in powder mixture on the surface of H13 die steel in this work. Microstructures and mechanical properties of the niobium layer are studied by adding different contents of rare earth (La) elements (0%, 1%, 3%, 5%). The results are as follows: the fabricated coating is mainly composed of NbC. And microhardness of coating first increases with the increase of rare earth (La), then decreases. When the rare earth (La) element content is 3%, the microstructure of coating is compact and uniform, and the thickness and microhardness are up to 7-9 μm and 1669 HV0.2 respectively. Under 5 N, 10 Hz, 5 min friction condition, with the increase of rare earth (La) content, the average friction coefficient of NbC coating/steel decreases gradually, and the wear resistance is improved. The addition of rare earth La into the packing powder mixture, the compactness, hardness and tribological properties of the coating are improved subsequently.

Keywords: lanthanide, niobium carbide coating, microstructure and properties

Study on formation mechanism of surface nanocrystalline layer during plasma nitriding of steel

Jiawei Yao

(Harbin Institute of Technology)

yjw0573@sina.com

Abstract: This article attempts to reveal the mechanism of nanocrystallization in the process of plasma nitriding and explain the occurrence of low-nitrogen compounds. The Gibbs free energy of the mixed Fe-Cr-N system is calculated by two thermodynamic models such as pseudo binary model and double sublattice model. The Gibbs free energy-composition curve of the Fe-Cr-N system showed a double potential, which confirms that the phase segregation in the ternary Fe-Cr-N systems is chemically spinodal nature at a suitable composition and temperature. Besides, the structures of different Cr equivalent (1/15, 1/11, 1/17) nitrogen-containing martensites and the structures of low nitrogen compounds are simulated by the first principle through Material Studio 8.0. This paper puts forward the nano-mechanism of Fe-Cr alloy steel that with the increase of N content the original large-size α' N occurs spinodal decomposition and forms nano-sized low-nitrogen compounds FeN_z and high nitrogen martensite α'' N, regulating the infiltration layer refinement at an appropriate temperature.

Keywords: plasma nitriding, thermodynamics calculation, first-principles calculation, spinodal decomposition, grain nanocrystallization

Quenching deformation control of ZL205A aluminum alloy by in situ formation of high strength gradient multiphase layer

Chen Lu¹, Yixue Wang¹, Mufu Yan¹, Hongya Fu¹, Chengsong Zhang², Fanyong Zhang³, Zhaobo Chen¹
(1. Harbin Institute of Technology; 2. Southwest Jiaotong University; 3. Hebei University of Technology)
sunnywang2013@sina.com, yanmufu@hit.edu.cn

Abstract: Aluminum-copper alloys are widely utilized in military, aerospace and aircraft industries for its light weight, excellent castability, superior corrosion resistance, as well as high specific strength after solution, quenching and age hardening treatments. However, the distortion occurring in the quenching process limits its application, especially for the large scale complicated workpieces. In this study, a novel duplex treatment combining the coating and nitriding is applied to the sections of the component that easy to deform during quenching. The temperature field and stress field of quenching process of this part are calculated by finite element method. The results show that a modified layer of great strength and stiffness is shaped on the sections easy to deform. The maximum radial deformation of the component can be reduced 65.7% compared with the original one, without significant increase in residual stress

Keywords: deformation control, ZL205A aluminum alloy, gradient multiphase layer, finite element simulation

Surface grain nanocrystallization of Fe-Cr-Ni alloy steel by plasma thermo-chemical treatment

R. L. Liu^{1,2}, M. F. Yan¹

(1. National Key Laboratory for Precision Hot Processing of Metals, School of Materials Science and Engineering, Harbin Institute of Technology, Harbin 150001, China;

2. Key Laboratory of Superlight Material and Surface Technology of Ministry of Education, College of Material Science and Chemical Engineering, Harbin Engineering University, Harbin 150001, China)
yanmufu@hit.edu.cn, liuruiliang@hrbeu.edu.cn

Abstract: The metal alloy with metastable state was plasma thermo-chemical treated with and without rare earths (RE) addition. The experimental results show that after plasma thermo-chemical treatments, the initial coarse-grained structure with 20-40 μm grain size of Fe-Cr-Ni alloy (17-4PH steel) could change into composition gradient nanoscale grains (as small as 5 nm) with random crystallographic orientations in plasma nitrocarburized layer. The hardness, modulus and wear resistance properties of nitrocarburized layer with nanoscale grains could be improved apparently. The present surface nanocrystallization method demonstrates the technological significance of metal alloy in improving traditional processing techniques and provides a new approach for surface nanocrystallizing of metal alloys.

Keywords: alloy steel, metastable state, plasma thermo-chemical diffusion treatment (PTCDT), surface grain nanocrystallization

Boriding treatment on alloyed white cast irons

Galtiere Corrêa Rêgo¹, José Benedito T. D. Rodrigues Neto¹, Amadeu N. Lombardi²,
George E. Totten³, Luiz C. Casteletti¹

(1. São Carlos Engineering School–University of São Paulo;

2. Federal Technological University of Paraná Londrina; 3. Portland State University, Portland, OR)
galtiere_9@hotmail.com

Abstract: Metallic materials are extensively applied in a wide variety of industries and high technology segments, essential to the production of goods and technological development. Therefore, there is a constant search for high performance materials, aiming to satisfy the requirements of different types of uses. In terms of application, due to the interaction with the environment, the surfaces of the materials are the most demanding, requiring in many cases high performance in terms of hardness, wear resistance and corrosion resistance. This can be obtained by means of surface treatments, with the production of layers with properties superior to those of the substrate. High chrome white cast irons consist of a class of materials widely used in castings, in applications that require moderate impact strength and high performance to abrasive, corrosive-abrasive and erosive wear. Typical applications of white cast iron are in the mining, milling, cement, steel mill industries in the manufacture of hot rolling mills, thermal power plants and agricultural machinery components used in the preparation of the land for planting. The high performance of the white cast irons can be achieved by means of heat treatments, inducing phase transformations or by means of surface treatments, seeking the production of layers with high hardness. The increase in wear resistance reduces maintenance costs and prolong the life of the material. The boriding thermo-chemical treatment is an effective method to increase the resistance to wear due to its high hardness and can be applied in a great variety of ferrous materials. This treatment consists in the production of layers of iron borides (FeB and Fe₂B), that can reach thicknesses of up to 380 µm and hardness of 2100 HV. In this process a substrate is subjected to a suitable mixture of boron-rich chemical compounds, which may be in solid, slurry, liquid or gaseous states. This method involves heating at high temperatures, ranging from 800 °C to 1100 °C for a time of 1 to 12 h. In the present work, layers of intermetallic borides were produced on substrates of a white cast iron alloy of the Fe-Cr-C system. The liquid borax method was used with a mixture consisting of borax (sodium borate - Na₂B₄O₇) and aluminum (10% by weight), at a temperature of 950 °C and treatment times of 2 and 4 h. The samples were cooled to room temperature, and then prepared by metallographic methods for observations and characterizations. The substrate and the layers were characterized by optical microscopy (OM), scanning electron microscopy (SEM), X-ray diffraction (XRD), micro-hardness vickers (HV) and microadhesive wear, with the tribological characteristics of the layers compared to that the substrate. The analyzes indicated the effectiveness of the boriding treatment in the white cast iron of the Fe-Cr-C system, producing layers with high resistance to wear when compared to the substrate. Layers thicknesses of approximately 30 µm for the two treatment times and hardness of 1530 HV and 1580 HV for 2 h and 4 h of treatments respectively were obtained.

Keywords: white cast irons, boriding, layers of boride

Rolling contact fatigue behavior of carbonitrided AISI 52100

high carbon bearing steel

Bin Liu¹, Bo Wang², Jianfeng Gu¹

(1. Shanghai Jiao Tong University; 2. Technical University of Denmark)

gujf@sjtu.edu.cn

Abstract: Rolling bearings are usually served under extreme conditions involving high speed, high cycling contact stress and contaminated lubrication in modern automobile industry. The contact fatigue has been convinced to be one of the most common failure modes of rolling bearings. Extensive studies have been undertaken in the aspects of materials and heat treatment process to extend the fatigue life. As a typical thermo-chemical surface modification technology, involving the diffusion of carbon and nitrogen into the substrate, gaseous carbonitriding has been considered as a cost-effective method to prolong the rolling contact fatigue life and improve the reliability of bearing subjected to operating condition of high cycling stress load and contaminated lubrication. Most investigations focus on the process optimization and the benefit of carbonitriding treatment to the low carbon bearing steels instead of the high carbon chromium bearing steel, such as AISI 52100 bearing steel. In order to clarify the internal relation between carbonitrided microstructure and contact fatigue performance of high carbon bearing steels, the microstructure observation, residual stress characterization, and contact fatigue behavior has been performed in the present work.

The specimens of 52100 high carbon bearing steel was employed and gaseous carbonitrided using carbon potential of 1.0% in flowing NH₃ (0.4 L/min) at 1108 K for 4 h, followed by tempering at 453 K for 2 h. Quenching and tempering (Q-T) without NH₃ intake was also adopted as a reference. Rolling contact fatigue (RCF) behavior of 52100 steel was performed on a ball-on-disc RCF tester at a peak pressure of 4.5 GPa under contaminated lubrication condition. The L10 and L50 lives were determined based on the two-parameter Weibull distribution, correspondingly. The microstructure, nitrogen concentration and fatigue fractures are systematically characterized pre- and post-RCF tests by TEM, EPMA and SEM, respectively.

The microstructure characterization results reveal that two types of nitrides ((Cr,Fe)₂N_{1-x}, CrN) precipitate in the surface layer, and a gradient nitrogen profile is obtained with a maximum concentration of 0.52 wt% at the top surface layer. XRD tests have been performed to obtain RS (residual stress) and RA (retained austenite) fraction in the carbonitrided specimen and Q-T specimens, respectively. It is clearly reveal that residual compressive stress has been induced in surface-modified sample with a maximum magnitude of 520 MPa, while a lower tensile stress (80 MPa) was generated in the latter sample. The RA fraction in the former specimen is about 36.2%, which is much higher than that in the latter specimen of 10.2%. Larger amplitude of compressive stresses is increased at the subsurface depth of 100 μm when the rolling contact cycling cycles up to 106 for the carbonitriding specimens as compared to the Q-T treated ones. Additionally, rolling contact load leads to greater volumetric fractions transformation of RA in carbonitrided specimens than the Q-T treated ones.

RCF tests show that the carbonitriding specimen has a 5 times of L10 fatigue life and 200% increasing L50 fatigue life under 90% confidence level, compared to the ones treated by Q-T process, which can be attributed to the higher fraction of RA and greater compressive RS at the surface. Fractographic analysis clearly indicates that the onset time of the cracks initiate from the subsurface is effectively retarded, as compared to the Q-T treated specimen.

Keywords: high carbon bearing steel, gaseous carbonitriding, residual stress, retained austenite, rolling contact fatigue

Evaluation of thermal fatigue property of surface-modified SKD 61 steel by gas nitriding and shot peening

Xingfeng Zhao¹, Bo Wang², Ming Qin¹, Jianfeng Gu²

(1. Hitachi (China) Research Development Corporation, Shanghai, China;

2. Department of Materials Science and Engineering, Shanghai Jiao Tong University, Shanghai, China)
gujf@sjtu.edu.cn

Abstract: A high pressure aluminum alloy die casting (HPDC) is a high series production process for producing of geometrically complex casings in tight dimensional tolerances and with high surface quality. During aluminum die casting, the die is repeatedly subjected to cyclic thermal and thermo-mechanical loadings, which causes surface damage. Thermal fatigue of hot work die steels has been convinced to be one the most common failure forms of aluminum alloy die casting process. Recent years, it has been common practice for many years to improve thermal fatigue resistance by some form of surface modification technologies such as gas nitriding and shot peening. Both gas nitriding and shot peening can increase the hardness and produce compressive residual stress, which should have a positive influence in enhancing thermal fatigue resistance.

In the present work, the hot work die steel SKD 61 was employed to investigate the effect of controlled gas nitriding, and shot peening plus gas nitriding on the hardness and residual stress, followed by evaluating the thermal fatigue resistance in accordance with the residual stress distribution characteristics, and initiation and propagation of the thermal cracks. With increasing the thermal cyclic numbers, both the width and length of the thermal cracks in three treated samples were increased. The proposed surface modification technologies had positive efforts in both inhabiting the thermal cracks initiating and propagating, as shown in Fig.1. The formation of the compound layer in the surface of traditional nitrided sample and its brittleness should be the main reason for the unique crack propagation behavior (Fig.1 and Fig.2). The excellent toughness of the compound-free layer contributed the slow growth of the thermal cracks in the controlled gas nitrided sample. In initiation stage of thermal fatigue test (100-300 cycles), no instability region was detected in the compound-free sample, whereas those in the compound layer and nitrided shot peened layer could be detected obviously. As the thermal fatigue cyclic number was up to 500, the compound-free layer and nitrided shot-peening sample showed large instability surface layer with thicknesses of approximately 155 μm and 160 μm , respectively. The surface residual compressive stress was decreased with increasing the thermal cyclic numbers. Residual stress results showed that the nitrided sample with a compound layer had the most excellent thermal fatigue resistance in initiation stage of thermal fatigue test. The increase of thermal fatigue test cycles significantly promoted the thickening of the crack but slightly influenced its elongation. A higher hardness distribution in cross-section of modified layer could effectively suppress the ingrowth of the crack. The expected research results will not only provide technique basis for the preparation of surface modified layer with satisfactory performance for the hot work die steels, but also help to broad the application of gas nitriding.

Keywords: gas nitriding, shot peening, SKD61 steel, thermal fatigue

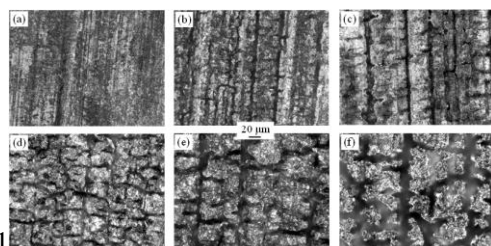


Fig.1

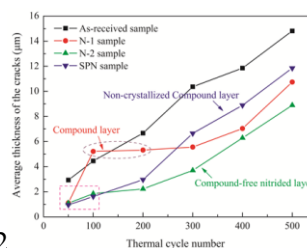


Fig.2

Fig.1 Optical micrographs of surface fatigue cracks in traditional nitrided samples after cyclic numbers from 50 to 500 times

Fig.2 Variation in average thickness of the cracks, as a function of thermal cycle numbers from 50 to 500 times

Thermal fatigue evaluation of AISI H13 steels surface modified by gas nitriding with pre- and post-shot peening

Bo Wang¹, Xingfeng Zhao², Ming Qin², Jianfeng Gu³

(1. Shanghai Jiao Tong University/Technical University of Denmark;

2. Hitachi (China) Research Development Corporation; 3. Shanghai Jiao Tong University)
gujf@sjtu.edu.cn

Abstract: In this work, the H13 hot work die steels were surface modified and experimentally evaluated in a homemade thermal fatigue simulation tester. Two types of nitrided compound layers, and compound-free layers with and without further deformation were prepared by a selection of surface modifications including traditional gas nitriding, controlled gas nitriding, gas nitriding with pre-shot peening, and controlled gas nitriding with post-shot peening. The results showed that the compound layer accelerated the surface thermal crack growth and promoted crack propagation along the surface as compared to the compound-free layer. The thermal crack longitudinal advancement in the sample nitrided with pre-shot peening had a tendency to be suppressed by the higher cross-sectional hardness distribution. The deformed compound-free nitrided layer showed the excellent thermal fatigue cracking resistance in both surface and cross-section, which was attributed to the good combination of hardness and toughness, as well as the expected superimposed compressive residual stress.

Keywords: hot work die steel, gas nitriding, thermal fatigue, thermal cracking

Microstructure and properties of plasma nitrided layer of aerospace TC4 alloy

Lina Tang, Tiande Zhang

(Shanghai Aerospace Equipment Manufacturer Co., Ltd.)

linatang149@163.com

Abstract: The pulse plasma nitriding for TC4 (Ti-6Al-4V) alloy widely used in aerospace was conducted at 760-850 °C for 15 h or 30 h in atmosphere of NH₃. The microstructure, microhardness, wear and corrosion resistances of the surface layers for the nitride specimens were characterized using optical microscopy (OM), X-ray diffraction (XRD), scanning electron microscopy (SEM), microhardness test, wear test, anodic polarization tests in 3.5% NaCl solution, respectively. Significant hardened layers bearing compound- and diffusion- layer can be obtained when TC4 alloy specimens are plasma nitrided at the experimental condition, and the compound layers mainly consist of TiN and Ti₂N phases. The thickness of nitride layer and the size of nitride particles on the surface increase with the increase of nitriding temperature and time. The phase transition in the surface layer of plasma nitrided TC4 alloy reveals the regulation of α -Ti α (N)-Ti Ti₂N TiN, while transporting Al element inwards and forming a Al-rich layer near the surface. The surface hardness of nitride layer of TC4 was improved to HV0.11056. The wear resistance of the TC4 alloy can be improved remarkably by plasma nitriding. The surface layer of TC4 alloy nitrided at 800 °C shows the lowest friction coefficient and the narrowest wear track. The nitride layers of TC4 alloys show excellent corrosion resistances after electrochemical corrosion test.

Keywords: plasma nitriding, TC4 alloy, microstructure, wear resistance

Electronic structures of InGaN₂ nanotubes

Yang Mao

(Xi'an Polytechnic University)

myang0217@gmail.com

Abstract: We investigate the electronic structures of InGaN₂ nanotubes (NTs) using first-principles calculations. It is found that all four types of InGaN₂ NTs, with the same diameter, have similar stability. The total energy of the per unit InGaN₂ NT depends on its diameter due to the curvature effect. The zigzag (armchair) InGaN₂ NTs have direct (indirect) band gaps. The band gap increases for all of the InGaN₂ NTs when their diameters increase. The valence band maximum (VBM) states of the InGaN₂ NTs are p-like states localised around N atoms. The p-like VBM states in zigzag (armchair) InGaN₂ NTs are perpendicular (parallel) to the tube axis.

Keywords: electronic structures, nanotube

Applications of XD super nitriding activator

Hongda Zheng

(DeYang Xingda Heat Treatment Technical Service, Deyang Sichuan, China)

ZHD8639@126.com

Abstract: “XD super nitriding activator” is showing us that is an extra-strong activator, as long as to enter the “XD super nitriding activator” into the current nitriding furnace, the nitriding hrs will be shortened more than 50%, and to meet to all the nitriding technical requirements. And it can make the nitration case depth be more than 0.80-1.00 mm within 100 hrs, which is an extra-depth nitration case. “XD super nitriding activator” will change our many knowledge of the nitriding theories, and will give the designers a new selection for nitration case depth in order to heighten the ability of parts to bear the load. It is a great progress for the nitriding technique of steel.

Keywords: nitriding activator, saving energy, environmental protection, high efficiency, extra-depth nitration case

Preparation and properties of nano-TiN co-deposited Ni-P composite coatings on TL084 copper alloy

Baofeng Chen, M. F. Yan
(Harbin Institute of Technology)
yanmufu@hit.edu.cn

Abstract: Ni-P-nanoTiN composite coatings were successfully prepared by electroless plating on TL084 copper alloy. Scanning electron microscope (SEM), energy dispersive spectrometer (EDS) and X-ray diffractometer (XRD) were jointly employed to characterize morphology, composition, structure and phase transformation behavior of the nano-composite coatings. Variations in hardness and wear resistance induced by the addition of these different amounts of nano TiN were also investigated and correlated with these microstructural characteristics. Compared with the conventional Ni-P coatings and original TL084 copper alloy, remarkable increases in hardness and wear resistance were noticed in the nanocomposite coatings, which can be ascribed to the nano TiN particles uniformly distributed in the Ni-P matrix.

Keywords: electroless, wear resistance, Ni-P

Low temperature plasma hardening of long and thin stainless steel tubes in the nuclear reactor

Cheng Zhao
(Qingdao Fengdong Heat Treatment Co., Ltd.)
c-zhao@126.com

Abstract: The long and thin stainless steel tubes ($\Phi 9.68$ mm \times 4000 mm) used in the nuclear reactor were hardened by plasma nitrocarburizing at low temperature. The hardened layer is the supersaturated solid solution of nitrogen and carbon atoms in the austenite (S phase) with high hardness and high corrosion resistance. All of the technical indicators can meet the requirements of nuclear power.

Keywords: long and thin stainless steel tubes, low temperature plasma nitrocarburizing, S phase